1988

Dynamics of Scroll Suction Process

Jeff J. Nieter
United Technologies Research Center

DYNAMICS OF SCROLL SUCTION PROCESS

Jeff J. Nieter
Associate Research Engineer
United Technologies Research Center
East Hartford, CT 06108

ABSTRACT

In this study, scroll compressor suction is modeled as a dynamic process using the differential continuity and steady, isentropic flow equations. Consequently, the effects of kinematics and flow dynamics are predicted and show that the suction gas actually starts to be compressed before the outer scroll wrap tips seal off the displacement volume of gas at the start of closed compression. Thus, it is possible to obtain a local volumetric efficiency, referenced to inlet conditions, of greater than 100 percent. The model is validated by comparison of the predicted suction pocket pressures with dynamic pressure measurements. Further, actual mass flow measurements confirm cyclic mass flow rates at suction which are greater than the traditional ideal value.

NOMENCLATURE

a	Base circle radius of scroll involute
A_{sp}	Inlet area into suction pockets
C_D	Discharge coefficient for flow into or out of suction pockets
E_{cv}	Energy contained within control volume
g	Gravitational acceleration
h	Height of scroll wrap
h_{in}, h_{out}	Enthalpy of gas entering, leaving control volume
h_{do}, h_{up}	Enthalpy of gas downstream, upstream of suction pockets inlet
m_{cv}	Mass of gas in suction pockets control volume
$\dot{m}_{in}, \dot{m}_{out}$	Mass flow rate of gas entering, leaving control volume
$\dot{m}_{sp}$	Mass flow rate of gas into or out of suction pockets
N	Number of pairs of compression pockets at start of closed compression
p_{sc}	Pressure in suction chamber
p_{sp}	Pressure in suction pockets
$\dot{Q}$	Rate of Heat transfer into control volume
$r_{fi,max}$	Radius to outer tip of fixed, inner wrap surface
$r_{mo/fi,max}$	Radius to outermost surface of moving wrap at $\phi_{fi,max}$
SOC	Start of closed compression process
SOS	Start of suction process
U_{cv}	Internal energy of gas in control volume
v_{in}, v_{out}	Velocity of gas entering, leaving control volume
V_{disp}	Displacement volume in outer pair of pockets at SOC
V_{sp}	Volume in pair of suction pockets
$\dot{W}$	Rate of boundary work done by control volume
z_{in}, z_{out}	Elevation of gas entering, leaving control volume

α Starting angle of involute

δ Thickness angle of wraps = 2α

$\phi_{fi,max}$ Polar angle to outer tip of fixed, inner wrap surface

η_{vs} Local volumetric efficiency at suction

θ Crank angle, or orbit angle position of orbiting scroll

λ_{max} Involute wrap angle to outer tip of fixed, outer wrap surface

$\lambda_{mo/fi,max}$ Involute wrap angle to outermost surface of moving wrap at $\phi_{fi,max}$

ρ Density of gas

INTRODUCTION

The unique performance characteristics of the scroll compressor have been demonstrated in a number of papers [1-7] in recent years. This paper demonstrates another unique characteristic: the passive supercharging effect which can occur during the scroll suction process for some speeds and suction manifold configurations. The basic operation of the scroll compressor has been sufficiently described in previous literature and, therefore, will not be reiterated here. However, the scroll suction process has not been adequately described as all previous work apparently assumes the suction process to be quasi-static filling of the suction pockets. Using that assumption, the cyclic mass flow rate at suction (before any leakage effects occur) is simply the traditional ideal value: the product of the gas density entering the suction pockets and the displacement volume created as the suction pockets are sealed off to form the outer pair of compression pockets. Such a model would predict the same cyclic mass flow rate at suction for all speeds and manifold configurations. In reality, the speed of compressor operation and the configuration of the suction manifold will affect gas flow into the suction pockets.

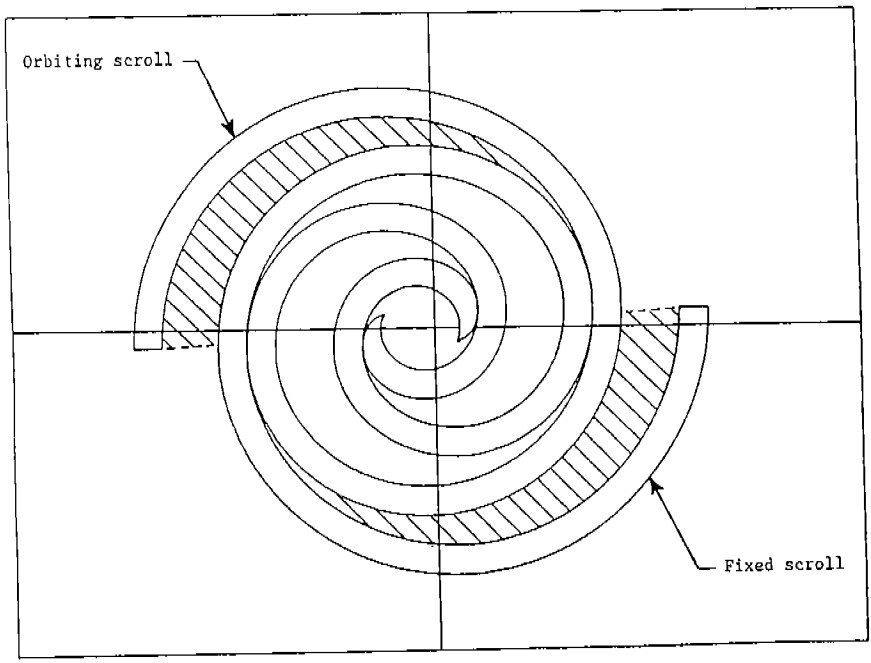

Figure 1 Typical pair of scroll suction pockets

ANALYTICAL MODEL

The suction gas flow in a scroll compressor is driven by the opening and closing of the pair of suction pockets. The pair of scroll suction pockets referred to are shown crosshatched in Fig. 1 for a typical scroll compressor geometry. The volume in the suction pockets, and the inlet cross-sectional area into the pockets, varies with crank angle as shown in Fig. 2 for such a geometry. During most of a scroll orbit cycle, the volume in the suction pockets increases and causes gas to be pulled into the pockets. But near the end of the orbit cycle, the volume in the pockets begins to gradually decrease until they are abruptly closed off at the end of one complete cycle. (Note the end of the suction process coincides with the start of the closed compression process.) The expression which describes the volume in the pair of scroll suction pockets as a function of crank angle is

$$V_{sp}(\theta) = \frac{h}{3} a^2 [\ [\ (\lambda_{max}-\delta)^3 - \lambda^3_{mo/fi,max} + 2\alpha^3 - \frac{\pi^3}{4}\ ] + (\pi-\delta)[\ 4\pi N(\theta-\pi N) - \theta^2 + \frac{\pi}{2}\alpha + 1 + \sin(\lambda_{mo/fi,max}+\theta-\alpha) - \lambda_{mo/fi,max}\cos(\lambda_{mo/fi,max}+\theta-\alpha)\ ]\ \} \quad (1)$$

while the equation describing inlet cross-sectional area into the suction pockets is

$$A_{sp}(\theta) = 2h[\ r_{fi,max} - r_{mo/fi,max}\ ] \quad (2)$$

(Variables used in these equations are further defined in the Appendix.)

To adequately model the scroll suction process, flow dynamics into the control volume of the suction pockets must be considered. The instantaneous mass of suction gas contained within the suction pockets control volume can be defined by the time differential continuity equation,

$$\frac{d}{dt}(m_{cv}) = \dot{m}_{sp} \quad (3)$$

The instantaneous mass flow rate of suction gas entering or leaving the control volume can be described using the steady, one-dimensional, isentropic flow equation,

$$\dot{m}_{sp} = C_D \rho A_{sp} \sqrt{2(h_{up}-h_{do})} \quad (4)$$

Also, the first law of thermodynamics on a time rate basis was applied to the suction pockets control volume,

$$\frac{d}{dt}(E_{cv}) = \dot{Q} - \dot{W} + \Sigma\, \dot{m}_{in}[\ h + \frac{v^2}{2} + gz\ ]_{in} - \Sigma\, \dot{m}_{out}[\ h + \frac{v^2}{2} + gz\ ]_{out} \quad (5)$$

For all equations, it is assumed that gas properties are uniform throughout each defined region, e.g. properties are uniform throughout the suction pockets. In applying Eq. (5), it is reasonable to assume the following terms are negligable and can be eliminated: heat transfer, boundary work, and kinetic and potential energies. One might question why the boundary work term

$$\dot{W} = (\ p_{sp}-p_{sc}\ )\ \frac{d}{dt}(V_{sp}) \quad (6)$$

can be neglected since the suction pockets volume changes considerably during each cycle. The reason is that the pressure difference across the suction pockets control volume boundary is quite small, consequently the product in the work term is negligable compared to the enthalpy terms. What is left then is the classic filling process energy equation

$$\frac{d}{dt}(U_{cv}) = \dot{m}_{sp} h_{up} \quad (7)$$

where it is assumed the time rate change of energy in the control volume equals the time rate change of internal gas energy. Initially, the energy equation in this form was used in the scroll suction process model. However, the initial analyses

using this equation produced unrealistic temperature rise predictions. Consequently, the energy equation was rejected in favor of assuming an isothermal scroll suction process since the temperature rise of the gas going from the suction chamber into the suction pockets should be small.

To utilize Eq. (4) for the mass flow rate into or out of the suction pockets, the conditions in the suction pockets and the suction chamber surrounding the orbiting scroll must be known. At the start of the suction cycle (SOS), the suction pockets do not exist per se' as their volume is zero at that instant. Immediately after the start of the cycle, the volume in the pockets is still quite small. During this early part of the suction process it can be assumed that quasi-static filling of the suction pockets takes place so that at any instant in time the volume in the pockets is completely filled with gas. (As a later comparison will show, there is very little difference between the instantaneous mass flow predicted by quasi-static filling and by the dynamic model presented here during the early part of the suction process.) This assumption allows the analysis to be initiated as conditions in the suction pockets can then be defined. Meanwhile, the conditions in the suction chamber can be determined by measurement or predicted using a seperate model. With the conditions in the suction pockets and suction chamber specified, the mass flow into the pockets can be computed. The continuity equation then determines the instantaneous mass in the suction pockets so that the conditions in the pockets can be defined for that time increment. This process is continued until the end of the suction cycle.

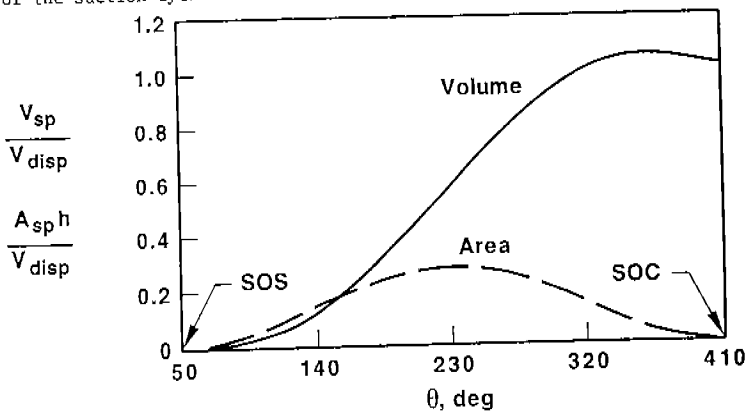

Figure 2 Volume and inlet area for pair of scroll suction pockets

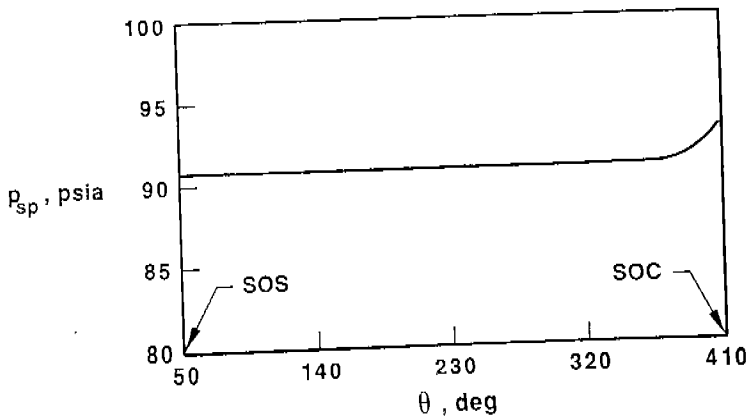

Figure 3 Suction pockets pressure predicted at ARI and 3500 rpm

SCROLL SUCTION CHARACTERISTICS

What results from using this scroll suction model is the ability to predict the pressure rise in the suction pockets that occurs as the volume in the pockets is reduced near the end of the suction process. This increase in suction pockets gas pressure indicates that early compression takes place before the displacement volume of gas is sealed off at the start of the actual closed compression process (SOC). Figure 3 shows the instantaneous pressure in the suction pockets predicted by this model for the typical geometry used in Fig. 2, and at the ARI condition and 3500 rpm. The predicted instantaneous mass flow rate into or out of the suction pockets (for the geometry and conditions of Fig. 3) is shown in Fig. 4 by the solid curve. The dashed curve in Fig. 4 indicates the instantaneous mass flow rate which would result if one assumes quasi-static filling for the entire process. Obviously, the dashed curve cannot represent reality since it assumes no flow dynamics and is discontinuous at the crank angle where the suction pockets are sealed off, a crank angle of 410 (= 50 + 360) deg. Therefore, besides predicting the early compression of suction gas, this suction process model also produces a continuous function for instantaneous mass flow rate at suction, which is important for accurate prediction of suction pressure pulsations in the manifold system.

Another important capability of this model is showing the effects of shaft speed on the suction efficiency. Suction efficiency refers to the ratio of the actual mass of suction gas sealed off in the displacement volume at SOC to the mass of gas sealed off after quasi-static ('ideal') filling. Instantaneous mass flow rates predicted by both methods are shown in Fig. 5 at 1750 rpm and Fig. 6 at 7000 rpm for the geometry and conditions used previously. Two effects can be seen in these figures during the suction process. The first effect occurs during the part of the cycle where the suction pockets volume increases (from SOS to about 270 deg. after SOS). During this part of the suction process, a slower shaft speed produces more complete (approaching quasi-static) filling of the suction pockets. As the speed increases, the suction pockets are less completely filled and suction efficiency suffers. The second effect occurs during the remaining part of the cycle where the suction pockets volume decreases until they are sealed off at SOC. During this part of the process, a faster shaft speed allows less gas to escape as the suction pockets volume decreases. However, at slower speeds, more gas is able to escape and the suction efficiency is reduced. These two effects produce opposing results, but for most operating speeds, gas which is kept from escaping during the second part of the process more than offsets any incomplete filling during the first part of the process. Consequently, the mass of gas contained at SOC for most speeds and operating conditions is greater than the traditional ideal value which assumes quasi-static filling for the entire process. Under some conditions the suction efficiency may be high enough that even after accounting for leakage effects, the local volumetric efficiency at suction could be greater than 100%. Local volumetric efficiency at suction refers to the ratio of delivered cyclic mass flow rate, which includes any leakage effects, to the ideal cyclic mass flow rate. Nevertheless, when shaft speed gets too high, incomplete filling during the first part of the process can offset the effect of gas which is kept from escaping during the second part of the process, resulting in a mass of gas at SOC which is less than the traditional ideal value.

A final capability to discuss about this model is predicting more accurately the effects of the suction manifold system on pressure pulsations as well as local volumetric efficiency. A detailed study on the subject of suction manifold tuning [8] is too involved to discuss here, but one example will be presented to show the potential effects. In Fig. 7, two local volumetric efficiency curves are shown versus speed. The solid curve is predicted for a realistic suction manifold configuration consisting mostly of the low-side shell passages and cavities. The dashed curve is predicted for an anechoic line attached to the suction chamber. It is apparent that a considerable increase in local volumetric efficiency can be gained by the use of such an anechoic line. Although in practice this may not be easily accomplished, it indicates the potential that exists for improving local volumetric efficiency by proper configuration of the suction manifold.

MODEL VALIDATION

The suction behavior described above, and the model in general, has been validated with data measured in the laboratory. Comparisons between measured and predicted suction pocket pressures at the ARI condition are shown in Figures 8-10

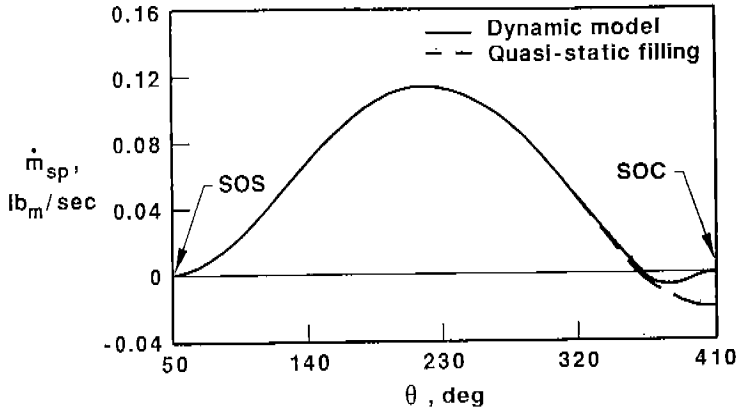

Figure 4 Mass flow rate into suction pockets predicted at ARI and 3500 rpm

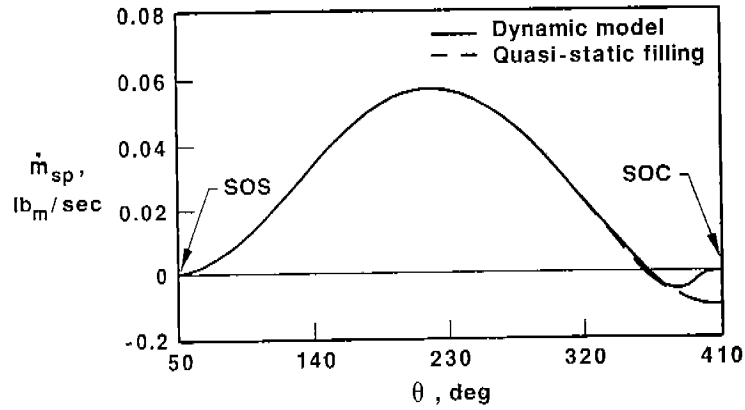

Figure 5 Mass flow rate into suction pockets predicted at ARI and 1750 rpm

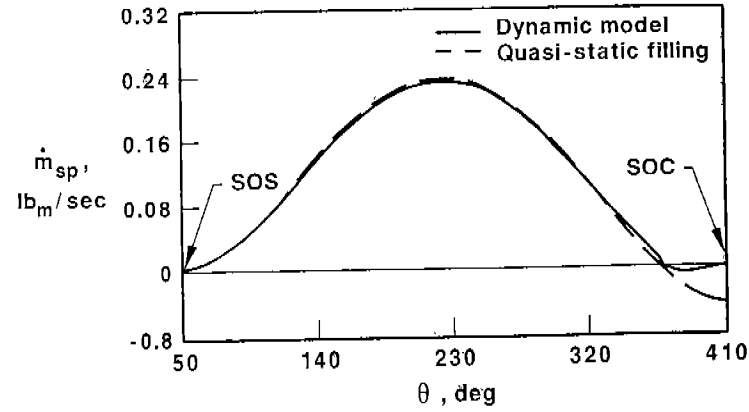

Figure 6 Mass flow rate into suction pockets predicted at ARI and 7000 rpm

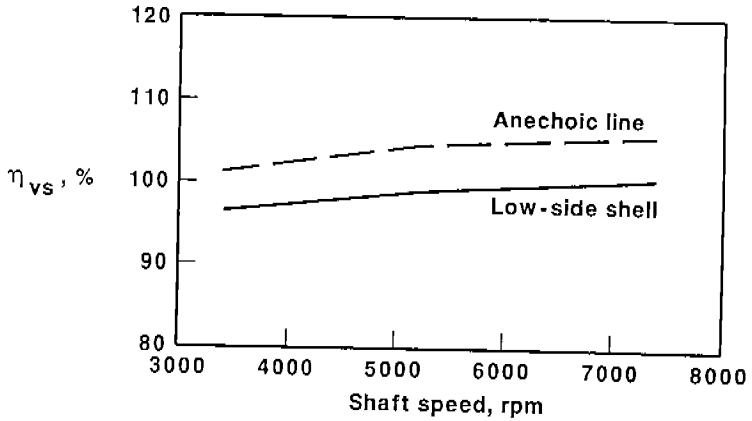

Figure 7 Local volumetric efficiency at suction for realistic low-side shell and for anechoic line

for the speeds of 3425 rpm, 5233 rpm, and 7034 rpm, respectively. (In Figures 8-10, as well as Fig. 11, predicted values are represented with solid curves and measured values are represented with dashed curves.) The measured pressure curves shown cover one complete 360 deg. cycle and were obtained from one of four dynamic pressure transducers installed in the fixed scroll at strategic locations which allowed most of the process to be covered from suction through closed compression and discharge (see Reference 9). Unfortunately, the first transducer did not cover the full 360 deg. suction process cycle; it starts at about 180 deg. after SOS and covers past SOC at 410 deg. The predicted curves begin at SOS and continue past the end of suction and into closed compression to the end of the measured data. The large initial step-like change and subsequent oscillations (more pronounced at higher speeds) in the measured pressures are caused by the orbiting scroll wrap uncovering the pressure transducer. While these comparisons all show excellent agreement, they also confirm the predicted early compression behavior which occurs just before SOC. One final comparison for this model is shown in Fig. 11 where measured local volumetric efficiency (referenced to suction chamber) is compared to that predicted. Again, the predicted behavior is confirmed as measured efficiency is above 100% at the higher speeds: a supercharging type of behavior.

CONCLUSIONS

A scroll suction process model consisting of the differential continuity equation and the steady, isentropic flow equation has revealed an interesting phenomenon which occurs during the suction of refrigerant gas: since the pressure in the suction pockets begins increasing before the start of the closed compression process, it is possible for the pressure at the start of closed compression to be greater than the suction chamber pressure. Such a condition may give rise to a local volumetric efficiency (referenced to the suction chamber conditions) of greater than 100%: a supercharging effect. This model predicts more accurately than any previously reported work the dynamic conditions occuring during the scroll suction process. Further, the model has been validated with measured data.

REFERENCES

1. Morishita, E., et al., "SCROLL COMPRESSOR ANALYTICAL MODEL", Proc. of the 1984 Intern. Compr. Eng. Conf. (Purdue), July 1984, pp. 487-495.
2. Tojo, K., et al., "A SCROLL COMPRESSOR FOR AIR CONDITIONERS", Proc. of the 1984 Intern. Compr. Eng. Conf. (Purdue), July 1984, pp. 496-503.
3. Bush, J.W., et al., "DIMENSIONAL OPTIMIZATION OF SCROLL COMPRESSORS", Proc. of the 1986 Intern. Compr. Eng. Conf. (Purdue), Aug. 1986, pp. 840-855.
4. Hayano, M., et al., "PERFORMANCE ANALYSIS OF SCROLL COMPRESSOR FOR AIR CONDITIONERS", Proc. of the 1986 Intern. Compr. Eng. Conf. (Purdue), Aug. 1986, pp. 856-871.

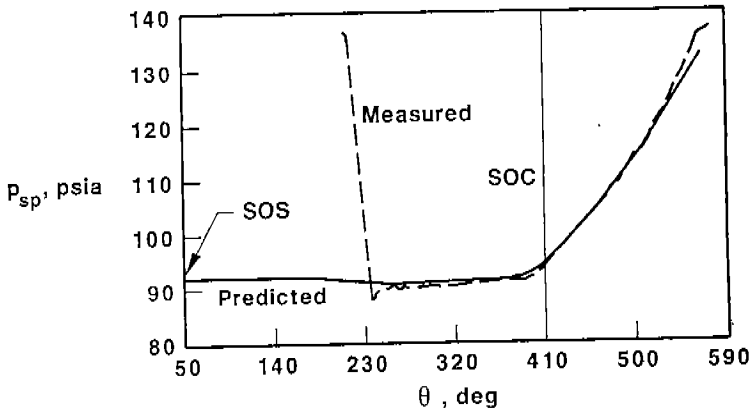

Figure 8 Comparison of predicted and measured suction pockets pressure at ARI and 3425 rpm

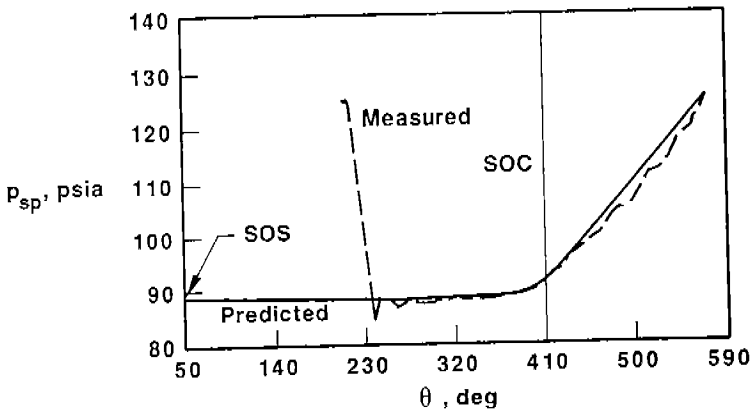

Figure 9 Comparison of predicted and measured suction pockets pressure at ARI and 5233 rpm

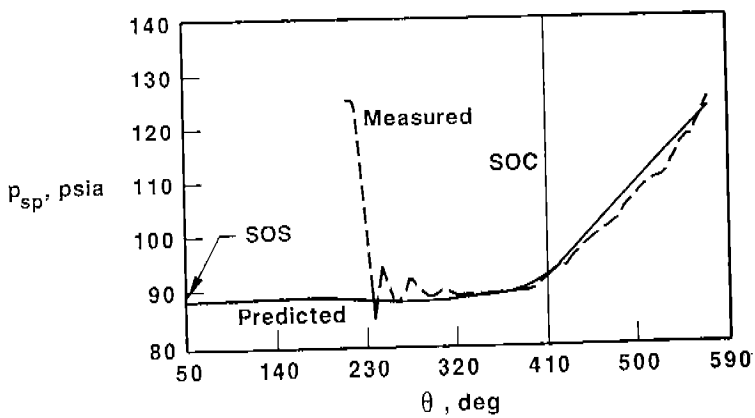

Figure 10 Comparison of predicted and measured suction pockets pressure at ARI and 7034 rpm

5. Tojo, K., et al., "COMPUTER MODELING OF SCROLL COMPRESSOR WITH SELF ADJUSTING BACK-PRESSURE MECHANISM", Proc. of the 1986 Intern. Compr. Eng. Conf. (Purdue), Aug. 1986, pp. 872-886.
6. Inaba, T., et al., "A SCROLL COMPRESSOR WITH SEALING MEANS AND LOW PRESSURE SIDE SHELL", Proc. of the 1986 Intern. Compr. Engr. Conf. (Purdue), Aug. 1986, pp. 887-900.
7. Ishii, N., et al., "A STUDY ON DYNAMIC BEHAVIOR OF A SCROLL COMPRESSOR", Proc. of the 1986 Intern. Compr. Eng. Conf. (Purdue), Aug. 1986, pp. 901-916.
8. Nieter, J.J. and Singh, R., "A COMPUTER SIMULATION STUDY OF COMPRESSOR TUNING PHENOMENA", Journal of Sound and Vibration, 1984, 97(3), 475-488.
9. DeBlois, R.L. and Stoeffler, R.C., "INSTRUMENTATION AND DATA ANALYSIS TECHNIQUES FOR SCROLL COMPRESSORS", Proc. of the 1988 Intern. Compr. Eng. Conf. (Purdue), July 1988.

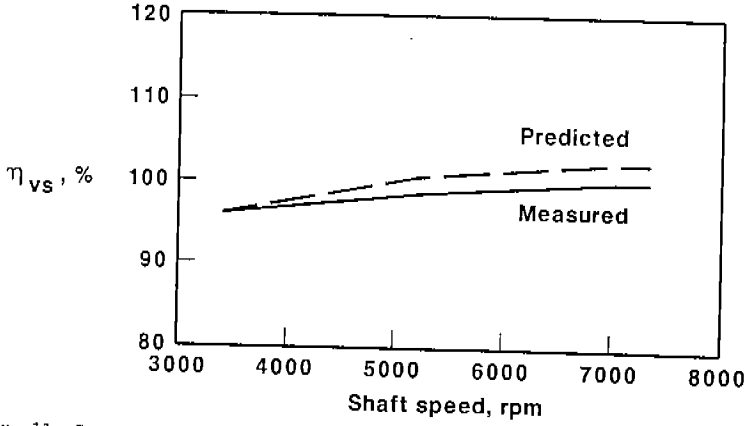

Figure 11 Comparison of predicted and measured local volumetric efficiency at suction for ARI condition

APPENDIX

Variables used in Equations (1) and (2) are further defined below as well as in Figures A1 and A2.

$$\phi_{fi,max} = (\lambda_{max}-\delta) - \tan^{-1}(\lambda_{max}-\delta) + \alpha \qquad (A1)$$

$$r_{fi,max} = a\sqrt{1 + (\lambda_{max}-\delta)^2} \qquad (A2)$$

$$r_{mo/fi,max} = a\sqrt{1 + \lambda^2_{mo/fi,max} + (\pi-\delta)^2 - 2(\pi-\delta)[\cos(\lambda_{mo/fi,max}+\theta-\alpha) + \lambda_{mo/fi,max}\sin(\lambda_{mo/fi,max}+\theta-\alpha)]} \qquad (A3)$$

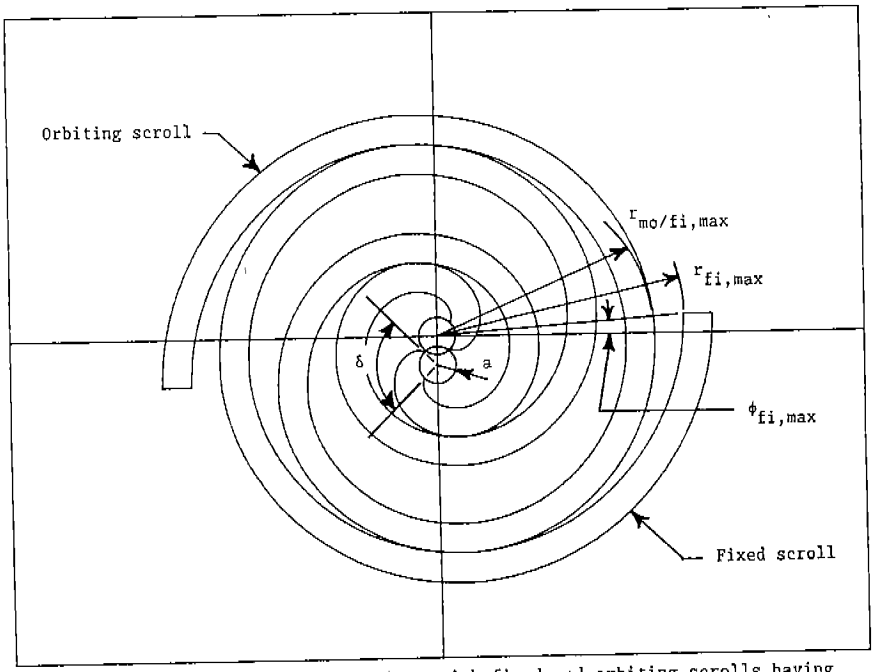

Figure A1 Geometric variables shown with fixed and orbiting scrolls having two full wraps (N=2)

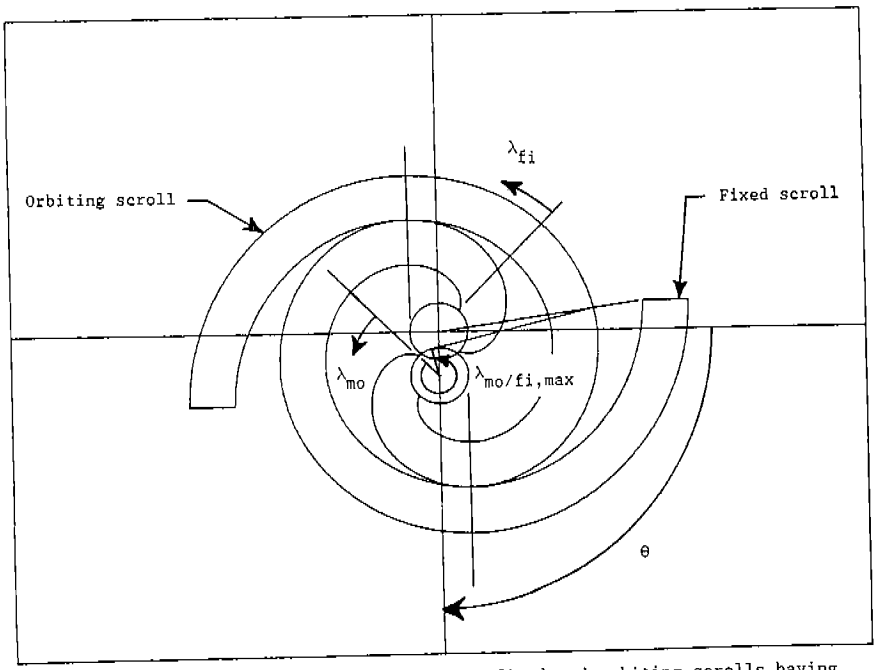

Figure A2 Geometric variables shown with fixed and orbiting scrolls having one full wrap (N=1)